

GREEN PHOTOCURABLE PHOSPHORUS CONTAINING COATINGS ON COTTON FABRICS

Zehra YILDIZ*

Received: 02.03.2023; revised: 22.06.2023; accepted:03.07.2023

Abstract: In this work, a bio-based, lightweight, coated cotton fabric by using a cleaner manufacturing method, “photocuring” was proposed in order to be used as an alternative to the conventional heat-, solvent-, and water-based outdoor textile (tarpaulin, tent, etc.) manufacturing. For this purpose, photocurable bio-based phosphorylated oligomer was synthesized with the reaction between a monomethacrylate functional phosphorus containing monomer and epoxidized soybean oil (ESBO). The synthesized phosphorylated ESBO (P-ESBO) oligomer was used in cotton fabric coatings in different proportions and photocured with UV light exposure. The effects of the amount of P-ESBO oligomer in the formulation on the crystalline morphology, mechanical, thermal, surface wettability, flammability, and abrasion resistance properties of the cotton fabrics were all searched. It was revealed that the increasing amount of P-ESBO oligomer in the formulation increases the drapeability and tensile strength of the fabrics with enhanced flame resist property by giving higher char yields. Besides, phosphorylated oligomer also acted as an adhesion promoter between the fabric surface and coating layer resulting a better abrasion resistance property.

Keywords: Soybean Oil, Photocuring, Ring Opening, Cotton Fabric, Phosphorus

Yeşil Kimya İle Fotokürlenebilir Fosfor İçerikli Pamuk Kumaş Kaplamaları

Öz: Bu çalışmada, biyo-esaslı, hafifletilmiş, kaplı pamuk kumaşların üretiminde, geleneksel ısı enerjisi, su ve çözücü kullanımını gerektiren dış mekân tekstilleri (tente, branda vb.) üretimine alternatif olabilecek, çevreci bir üretim yöntemi olan fotokürleme kullanılması hedeflenmiştir. Bu amaçla, fotokürlenebilir, biyo-esaslı fosforlanmış bir oligomer, monometakrilat fonksiyonelliği olan fosfor içerikli bir oligomer ve epokside edilmiş soya fasulyesi yağı (ESBO) reaksiyonu ile sentezlenmiştir. Sentezlenen fosforlanmış ESBO oligomeri (P-ESBO) farklı oranlarda kaplama formülasyonlarında kullanılmıştır. Daha sonra kaplanan bu formülasyonlar pamuk kumaş üzerine uygulanmış ve UV ile kürlenmiştir. Formülasyondaki P-ESBO oligomer oranının, pamuk kumaşın kristal morfolojisi, mekanik, termal, yüzey ıslanabilirliği, alev alma ve aşınma dayanımı özelliklerine olan etkileri incelenmiştir. Elde edilen bulgular ışığında, formülasyondaki P-ESBO oligomer artışının kumaşların dökümlülüğü ve kopma mukavemetini arttırdığı, alev dayanımını ise daha yüksek piroliz ürünleri vererek geliştirdiği gözlenmiştir. Bununla birlikte, fosfor içerikli oligomerin pamuk kumaş ve kaplama formülasyonu arasında yapışmayı artırıcı bir rol oynadığı ve böylece kaplı kumaşların aşınma dayanımını iyileştirdiği görülmüştür.

Anahtar Kelimeler: Soya Fasulyesi Yağı, Fotokürleme, Halka Açılma, Pamuk Kumaş, Fosfor

* Marmara University, Faculty of Technology, Department of Textile Engineering, Aydınevler mah. Uyanık sok., RTE Campus, T1/319, Maltepe, 34840, Kadıköy/Istanbul/Turkey

zehra.yildiz@marmara.edu.tr

1. INTRODUCTION

Vegetable oils are accepted as a great candidate to reduce the usage of petrochemicals in polymer synthesis due to the being abundant, biodegradable, renewable, non-toxic, non-depletable, and cheap. Among vegetable oils, soybean oil is favored with low toxicity, and possessing five unsaturated groups on its backbone which allow to the reactions with some chemical species. Epoxidation is the most common modification reaction in literature that involves the formation of oxirane ring in the presence of hydrogen peroxide and a catalyst. The intentionally formed oxirane rings on the soybean oil backbone, allows to further reactions generally by acids, amines etc. in order to be used as a starting material in the synthesis of specially designed polymers (Alam, Akram et al. 2014, Islam, Beg et al. 2014, Zhang, Garrison et al. 2017, Chen, Cai et al. 2019, Cai, Chen et al. 2020).

Photocuring technology is favored due to the several reasons; requiring none/less solvent, rapid crosslinking mechanism even at room temperature, high curing rates with high optical clarity, high scratch resistance with a controlled elasticity, applicability on complex shaped materials etc. Considering all the mentioned advantages, photocuring represents an environmentally friendly coating technique in comparison with the conventional thermal and solvent based coating technologies (Bajpai, Shukla et al. 2002, Moon, Shul et al. 2005, Hwang, Kim et al. 2009, Habib and Bajpai 2010, Sung and Kim 2013). In literature, in order to prepare photocurable coating formulations, the oxirane ring of epoxidized soybean oil (ESBO) has been reacted by cashew nutshell liquid, vinyl phosphonic, methacrylic, and acrylic acids then they have been used for various applications such as 3D printing, flame resist coatings, oil absorbing materials etc. (Baştürk, İnan et al. 2013, Li, Ma et al. 2017, Liu, Luo et al. 2017). Most of the photocurable coatings are highly flammable as they mainly consist of carbon, oxygen, and hydrogen atoms. In literature, a number of studies have been made regarding the inclusion of phosphorus containing chemical species to obtain a flame resist property. Besides the flame resistance effect, phosphorus based coatings also present anticorrosive and adhesion promoter properties (Chen, Song et al. 2011, Luangtriratana, Kandola et al. 2015, Kowalczyk, Kowalczyk et al. 2018).

In textile industry, polymeric fabric coatings are being applied to enhance some properties such as thermal stability, mechanical, wettability, hydrophilicity, drapeability etc. or to give some additional functionalities like antibacterial, antifungal, resistance to flame, chemicals, mold, sharp objects, heat and so on. These polymeric coatings involve the usage of conventional solvent-, water-, and thermal-based coating techniques that possess harmful effects on human health and nature. The coating substrate is generally a petroleum based non-renewable polymeric structure for instance; acrylic acid, ethylene vinyl acetate (EVA), polyvinyl chloride (PVC), and polyurethane (PU) etc. (Salim, Abas et al. 2018, Aliverdipour, Ezazshahabi et al. 2020). The main aim of this study is the manufacturing of lightweight coated cotton fabrics with enhanced mechanical and thermal properties by using a bio-based starting material (soybean oil), instead of petroleum based chemicals, in the synthesis of the phosphorous containing ESBO (denoted as P-ESBO) oligomer via an environmentally friendly technique (photocuring). A specialty designed phosphorus containing reactive monomer having methacrylate functionality was used to chemically modify the ESBO backbone. Then, the obtained P-ESBO oligomer was chemically analyzed by ^1H NMR and FTIR spectroscopies, respectively. Coating formulations were prepared by using the synthesized P-ESBO oligomer, a photo initiator, and a reactive diluent. Cotton fabrics were coated by the prepared coating formulations through dip coating, then photocured by UV light exposure. The effects of the amount of P-ESBO oligomer in the formulation on the crystalline/amorphous regions, thermal transitions,

flammability, surface wettability, abrasion resistance, and mechanical characteristics of the coated photocured cotton fabrics were all searched.

2. EXPERIMENTAL

2.1. Materials

ESBO (MW=952 g/mole, EEW=232 g/equiv.), perchloric acid (HClO₄), potassium hydroxide (KOH), 1,6-hexanediol diacrylate (HDDA), methyl acrylate (MA), tetraethylammonium bromide, acetic acid, indicators (crystal violet and phenolphthalein), dibutyltin dilaurate (T12, catalyst), hydroquinone (HQ, inhibitor), and ethanol were all purchased from Merck and used without any purification. 1-hydroxycyclohexyl phenyl ketone (Irgacure 184) was used as photoinitiator. Monomethacrylate functional phosphorus containing monomer, commercially known as Sipomer PAM-200, was received from Solvay. Cotton fabrics (woven in plain structure, bleached and desized, 135 g/m² in weight, 42 warp/cm, 30 weft/cm) were supplied from Sarteks Mensucat, Bursa, Turkey.

2.2. P-ESBO Oligomer Synthesis

Synthesis of the phosphorous containing ESBO (P-ESBO) oligomer was performed similarly in the authors' previous study (Yildiz 2023). The reaction was set in a three-necked round-bottom glass flask, by using a magnetic stirrer, a condenser, under nitrogen inert atmosphere. Sipomer PAM-200 is a specialty purpose monomer which is being used to improve the adhesion of coating formulations on various surfaces. Besides, here it was used as the phosphorus source for the oligomer in order to enhance the thermal properties of the coating formulations. Considering the epoxy equivalent weight (EEW) of ESBO (232 g/equiv.), the ESBO:Sipomer PAM-200 molar ratio was set as 1:0.5. The scheme of the reaction can be observed in Figure 1. First, ESBO and Sipomer PAM-200 were loaded into the flask and stirred at 200 rpm. Then HDDA (30% out of the total amount of monomethacrylate functional phosphorus containing monomer and ESBO), 300 ppm HQ and 3 drops of T12 were all loaded into the flask. The reaction mixture was stirred for 30 min at room temperature and for 1.5 h at 50 °C. The completion of the reaction was followed by checking the EEW and acid value (AV) in every 15 min via ASTM titration procedure. Then it was ended when a constant EEW and AV were obtained. During the reaction, the oxirane groups of ESBO were opened by the hydroxyl groups of Sipomer PAM-200 which was initiated by the nucleophilic attack of the catalyst (T12) resulting with the formation of phosphonium betaine. A proton of Sipomer PAM-200 was attached to the betaine then an ester bonding was formed by the effect of carboxylate anion on the electrophilic carbon of the phosphorus (Su, Cheng et al. 2012).

2.3. Preparation and Application of the Coating Formulations

Coating formulations were prepared by using the phosphorylated ESBO oligomer and MA (reactive diluent) in various proportions, and 3 % photo initiator. In order to lower the viscosity of the coating formulation for a better wettability property on the fabric surface, the formulation was heated above room temperature (~40 °C). Table 1 shows the composition of coating formulations with the designated sample codes, i.e., sample B means the fabric that is coated by the coating formulation of 75 % MA, 25 % P-ESBO oligomer, and 3 % photo initiator (out of the total MA+P-ESBO amount). Cotton fabrics were cut in 30x6 cm dimensions that are require to perform the tensile test, and then they were dipped into the coating formulation for 5 min. The excess of the coating formulation was dissipated from the fabric by a squeezing roller in 500 g weight. In order to prevent the oxygen inhibition during the photocuring stage, dip-coated fabrics were put into a transparent ziplock PE

bags. Cole-Parmer UVP Longwave UV Crosslinker cabinet (115 VAC model) was employed for the photocuring stage from both sides of the fabric for 3 min. Considering the formulation uptake capacity of cotton fabrics based on our previous studies in dip-coating bath, at around 30 % weight uptake was achieved on coated photocured cotton fabrics without any agglomeration. The schematic representation of the coating process also was illustrated in Figure 1.

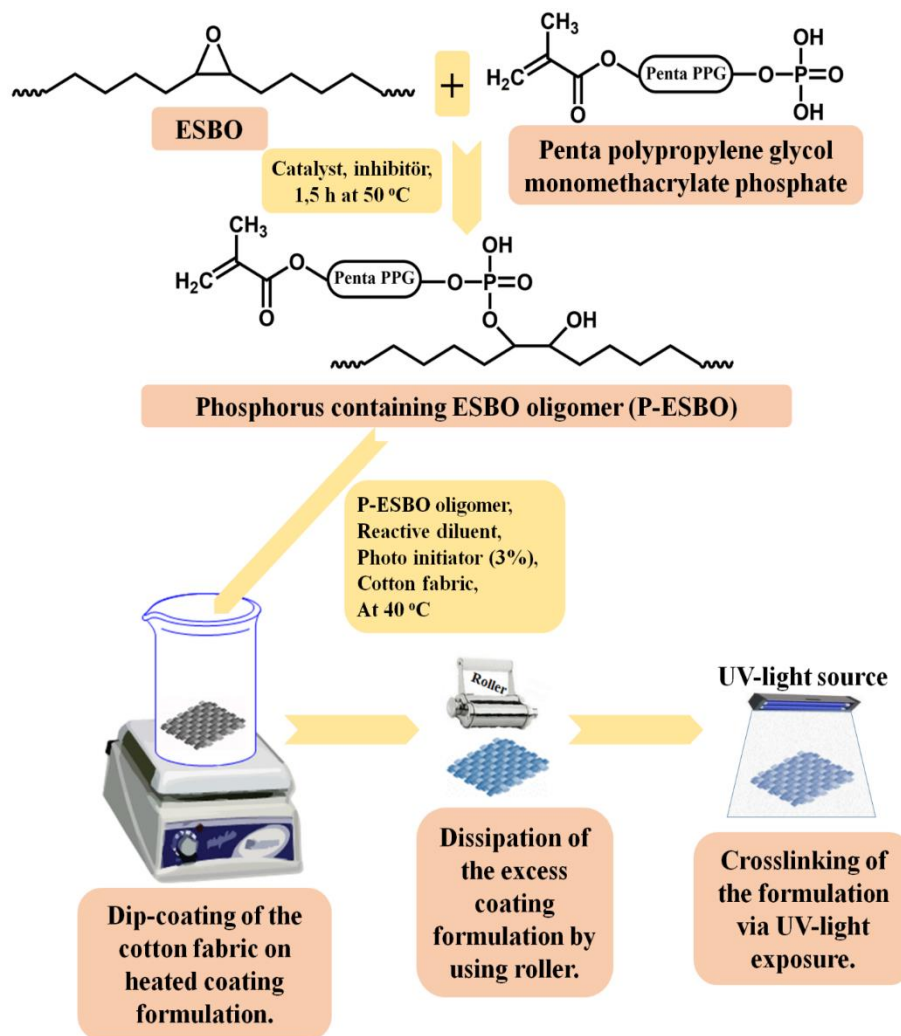


Figure 1:
Scheme of the reaction and coating process.

Table 1. Compositions of the coating formulations with the sample codes.

Sample Codes	MA (%)	P-ESBO (%)	Photo Initiator (%)
A	100	0	
B	75	25	
C	50	50	3
D	25	75	
E	0	100	

2.4. Characterization

The chemical structure of the phosphorylated ESBO oligomer was analyzed by using Fourier transform infrared (FTIR) spectroscopy (Perkin Elmer Spectrum-100) equipped with an ATR sampling holder and proton nuclear magnetic resonance (^1H NMR) spectroscopy (Bruker AMX 500 MHz NMR, solvent: dimethyl sulfoxide, with internal reference of the tetramethylsilane), respectively. X-ray diffraction (XRD) patterns of the coated photocured fabrics were obtained by using D/Max-BR diffractometer (at 30 mA, 40 mV over a 2θ range of $10\text{-}80^\circ$ at a rate of $2^\circ/\text{min}$) to investigate the amorphous and crystalline phases. OriginPro 7.0 software was employed to monitor the XRD patterns. Thermal transitions and stability of the coated photocured fabrics were observed by simultaneous TG/DSC (thermogravimetry/differential scanning calorimetry) measurement (Netzsch DSC 204) in an inert atmosphere with a $20^\circ\text{C}/\text{min}$ heating rate till 600°C . The flammability behavior of the coated photocured fabrics was investigated by using the limiting oxygen index (LOI) test which gives the required amount of oxygen for a three-minute-flame to burn the whole sample (2019). The existence and uniformity of the coating layer on the fabric surface was observed by using scanning electron microscopy (SEM, ZEISS Ltd, JSM-5910LV). In order to observe the wettability nature of the coated fabrics absorbency test was employed based on the measuring the disappearance time of a water droplet on the coated fabric surface that is recorded by a chronometer. The hydrophobicity of the coated fabrics was investigated by contact angle measurement (Fibro System Ab, Gardco PGX+goniometer) equipped with a camera. The adhesion between the coating layer and fabric surface, was investigated by using an abrasion resistance test on a Martindale abrasion and pilling device. Instron 4411 tensile testing machine was employed to record the tensile strength and elongation at break values of the coated photocured fabrics. The flexibility and resilience behavior of the coated photocured fabrics were searched by using the crease recovery angle test (Gan 2021). Samples in $15\text{ mm} \times 40\text{ mm}$ dimensions were horizontally folded and then put under a 10 N force for 5 min in a crease recovery angle tester. The angle between the folded layers gives the crease recovery angle of the samples.

3. RESULTS AND DISCUSSION

3.1. Oligomer Properties

The synthesized P-ESBO oligomer was characterized by titration methods periodically by means of AV and EEW during the reaction. AV shows the KOH amount (mg) that is needed to neutralize a 1 g of P-ESBO oligomer. EEW gives the amount of P-ESBO oligomer (g) that contains a 1 gram equivalent of epoxide group. At the beginning of the reaction the EEW and AV were found as 232 g/Eq. and 30.7 mgKOH/g, respectively. These results decreased gradually till the constant values (7.53 mgKOH/g and 380 g/Eq.) were obtained. The decline of these values proves the completion of the reaction due to the depletion of the epoxide groups of ESBO by the Sipomer PAM-200 oligomer. The chemical structures of ESBO and P-ESBO oligomers were also characterized by FTIR and ^1H

NMR spectroscopies. Figure 2 shows the FTIR spectra of the oligomers. Accordingly, the characteristic ester peaks of triglyceride structure were observed at 1740 cm^{-1} in both spectra. The bands at around $2840\text{--}2980\text{ cm}^{-1}$ were attributed to the aliphatic $-\text{CH}_2-$ groups of ESBO (Çakmakçı 2017). The oxirane peaks of ESBO were appeared at 825 cm^{-1} and 905 cm^{-1} . These peaks were disappeared in the P-ESBO spectra due to the ring opening of epoxide groups. Furthermore, a newly formed C-H bending vibration peak at 809 cm^{-1} in P-ESBO spectra also supported the ring opening reaction. In the spectra of P-ESBO, the peaks at 996 cm^{-1} (P-O), 1243 cm^{-1} (P=O), and 1100 cm^{-1} (phosphate ester vibration) were all proved the inclusion of monomethacrylate functional phosphorus containing monomer to the chemical structure of P-ESBO oligomer. The acrylate peaks ($\text{CH}=\text{CH}_2$) at 1619 cm^{-1} and 1636 cm^{-1} were also formed in the spectra of P-ESBO oligomer after the synthesis reaction (Shi, Wang et al. 2006, Liu, Xu et al. 2012, Baştürk, İnan et al. 2013, Ugur, Kılıç et al. 2014, Wu, Liu et al. 2019).

The ^1H NMR spectra of the P-ESBO oligomer in CDCl_3 was given in Figure 3. Accordingly, the monomethacrylate functionality of the phosphorylated ESBO oligomer can be observed by the proton peaks at $5.59\text{--}5.60\text{ ppm}$ ($\text{C}(\text{CH}_3)=\text{CH}_2$ in trans position) and $6.10\text{--}6.18\text{ ppm}$ ($\text{C}(\text{CH}_3)=\text{CH}_2$ in cis position), respectively. Methyl protons of methacrylate unit, penta PPG, and saturated triglyceride backbone were all recorded at $0.82\text{--}1.45\text{ ppm}$ region. The peaks at $4.1\text{--}4.3\text{ ppm}$ and $5.1\text{--}5.3\text{ ppm}$ were attributed to the characteristic methine and methylene protons of triglyceride backbone. The protons in allylic position were observed at 2.4 ppm . The methylene protons of the ESBO backbone were seen at $1.45\text{--}1.7\text{ ppm}$ region. The peaks at $2.8\text{--}3.2\text{ ppm}$ region were assigned to the aliphatic $-\text{OH}$ protons of phosphorus groups. Due to the epoxide ring opening reaction, the methine peak at 4.35 ppm and the hydroxyl proton peak at $3.3\text{--}3.6\text{ ppm}$ region were all observed (Liu, Wang et al. 2011, Uysal, Acik et al. 2017, Wu, Hu et al. 2018).

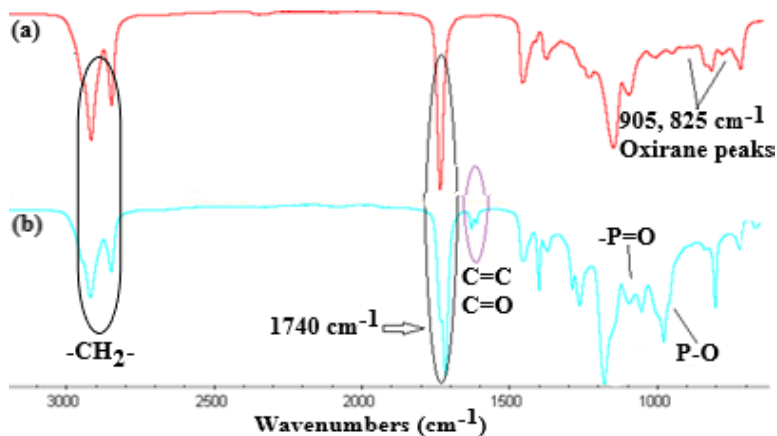


Figure 2:
FTIR spectra of (a) ESBO, (b) P-ESBO.

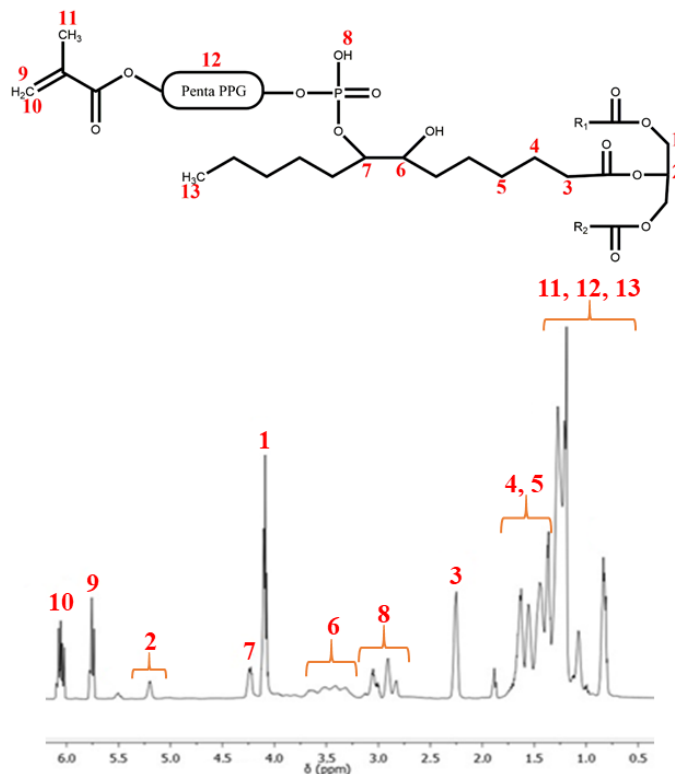


Figure 3:
¹H NMR spectra of the P-ESBO oligomer.

3.2. XRD Analysis

The cellulose I is the most abundant cellulose type in nature and its' structure composes of two distinct crystal shapes namely cellulose I α and cellulose I β . The cellulose I β is the dominant crystallite structure of cellulose in cotton so the Figure 4 illustrates the XRD patterns of cellulose I β structure in raw fabric and in fabrics by means of each photocurable coatings (Nam, French et al. 2016). The application of photocurable coating changed the intensities of characteristic XRD peaks of raw cotton fabric at 14.7°, 16.8°, and 22.7° due to the displacement of cellulose crystals. The penetration of the coating layer into the cellulose fibrils affected the crystal structure of cellulose resulting wider peaks which are associated with increasing amorphous character (Gupta, Uniyal et al. 2013). In XRD patterns, wide peaks are responsible of the amorphous areas whereas narrow peaks prove the existence of crystalline areas (Rowe and Brewer 2018). Accordingly, the characteristic cellulose peaks became broader from the sample A to the sample E. In other words, increasing amount of the synthesized P-ESBO oligomer in the coating formulation increased the overall amorphous regions. This result is stemming from the long flexible aliphatic groups of polyol and pendant methyl groups of penta PPG that increase the free volume of the chains via inhibiting the formation of a close packed crystal structure (Kaczmarek and Vuković-Kwiatkowska 2012, Kalita 2018).

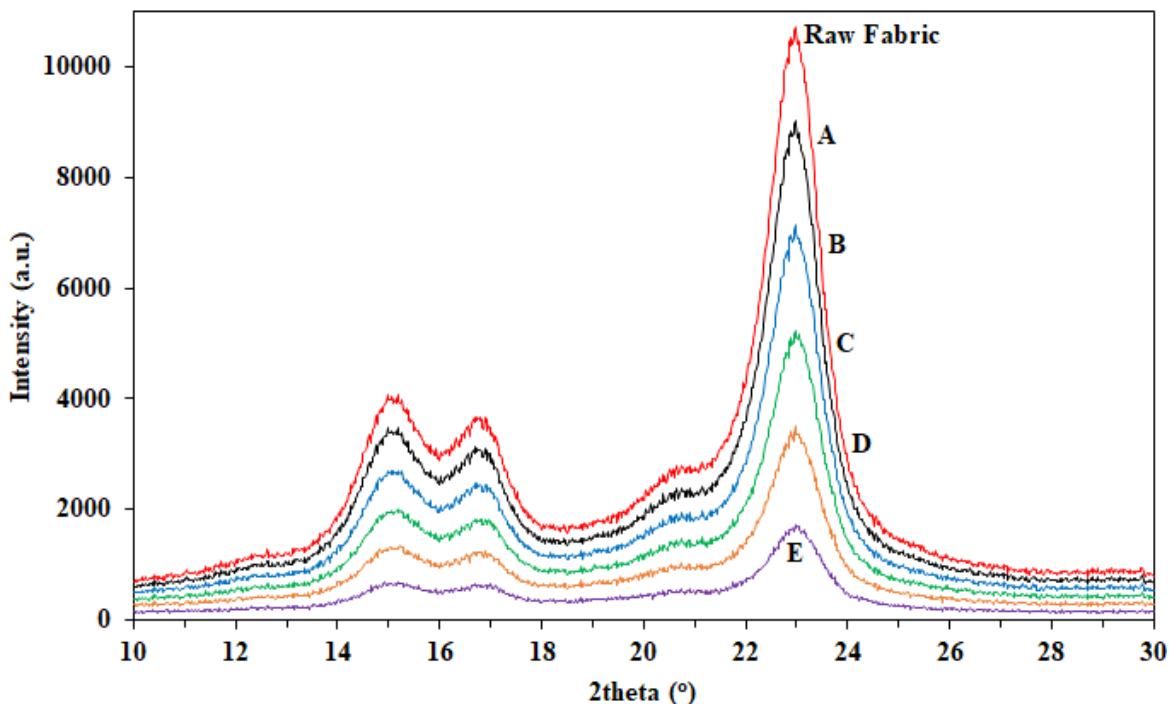


Figure 4:
XRD patterns of raw fabric and each coated photocured fabric samples.

3.3. TG-DSC Analysis

Figure 5 illustrates the curves of TG-DSC analysis of the raw fabric and photocured fabrics by means of each coating formulation. The TG data of the raw fabric and coated photocured fabrics were listed in Table 2. The weight loss below 100 °C in TG curves is related to the moisture evaporation that is adsorbed by cotton fabrics. Considering the thermal transitions of the samples, due to the aliphatic character of P-ESBO oligomer, which gives chain movement activity, thermal stability decreases with increasing amount of P-ESBO oligomer in the coating formulation. Thus the sample of E showed the least T_d value (Chen, Yang et al. 2013). Due to the changes on the neat intermolecular hydrogen bonding structure of cellulose crystallites, the T_g of raw fabric first decreased for the samples of A, B, and C then slightly increased after the application of coating formulations. Furthermore, the characteristic T_d peak of cellulose at 355 °C was also affected from the reconfiguration of hydrogen bonding resulting lower decomposition temperatures in photo-cured coated samples (Yang, Zeng et al. 2014). Under nitrogen atmosphere, carbonization takes place via pyrolysis of the samples resulting the formation of char. A remarkable increase was observed in the char yield at 600 °C through the sample of A to E, due to the increasing amount of P-ESBO oligomer in the coating formulation. This result can be supported by the changes in pyrolysis mechanism of the cellulose through dehydration step instead of the levoglucosan formation resulting greater amounts of char. Additionally, the phosphorylated oligomer prevents degradation of the coated fabric resulting a higher char yields that inhibits the spread of heat and pyrolysis products through the sample (Gao, Wu et al. 2009, Yildiz, Onen et al. 2016, Xu, Wang et al. 2017, Gong, Zhou et al. 2020).

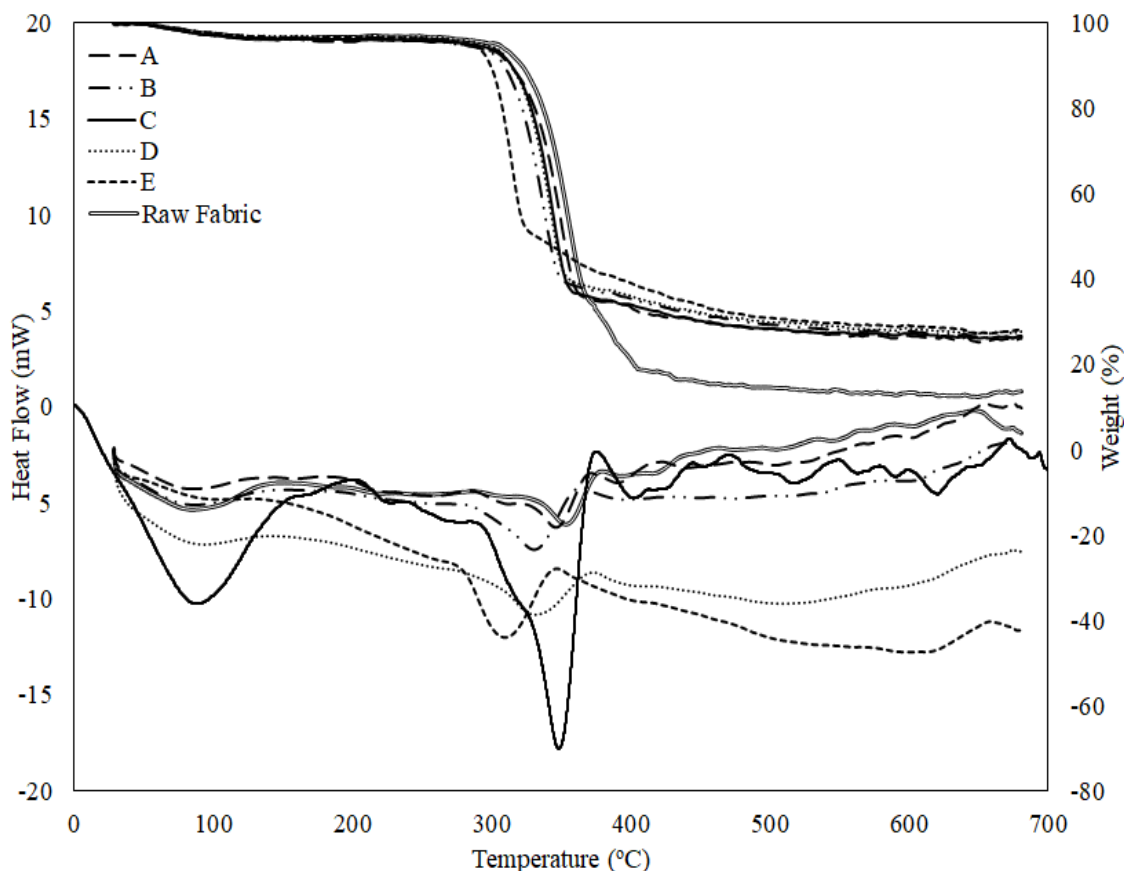


Figure 5:
TG-DSC curves of raw fabric and each coated photocured fabric sample.

Table 2. Thermogravimetric data of raw fabric and coated photocured fabrics for each formulation.

Sample Codes	T _g (°C)	T _d (°C)	Weight Loss Temperature		Residue at 400°C (%)	Char Yield (%)
			5%	50%		
Raw Fabric	88	355	305	357	21	13.7
A	81	351	280	351	33	26.1
B	78	332	276	340	35	26.7
C	80	340	286	346	34	26.6
D	93	325	295	345	36	27.7
E	102	309	285	332	39	28.1

3.4. Flammability Behavior of the Coated Photocured Fabrics

The LOI test is commonly used to evaluate the flammability characteristic of polymeric coatings. The LOI test results and the sample images after the test were given in Figure 6. According to the results, the increasing amount of phosphorylated oligomer (P-ESBO) through the sample A to E gradually increases the LOI values of coated photocured fabrics. As noted in the TG-DSC section, P-

ESBO oligomer is responsible of the char formation that prevents the spread of heat and pyrolysis products through the sample resulting a flame resist property. Due to the highest P-ESBO oligomer content, the sample E showed the best LOI value of 25 by giving the highest amount of char formation. These results also consistent with the TG-DSC curves in Figure 6, that also support the char formation via phosphorus content (Yildiz, Onen et al. 2016, Çakmakçı 2017).







Sample Codes	Raw Fabric	A	B	C	D	E
Images After LOI Test						
LOI Values	19	20	21.7	22.9	24.1	25

Figure 6:

LOI values and images of the raw fabric and coated photocured fabrics after the test.

3.5. Surface Morphology, Wettability, and Abrasion Resistance

The surfaces of coated photocured fabrics were evaluated in terms of the morphology, wettability, and abrasion resistance performances. The SEM images of raw fabric and the sample of E in 2k magnification were illustrated in Figure 7. SEM analysis was employed to observe the uniform dissipation of the coating layer through the fiber surface. Accordingly, the rough fiber surface in raw cotton fabric gained a smooth look in sample E due to the presence of coating layer on fiber surface. The coating layer was well-dissipated on fiber surface without any agglomeration.

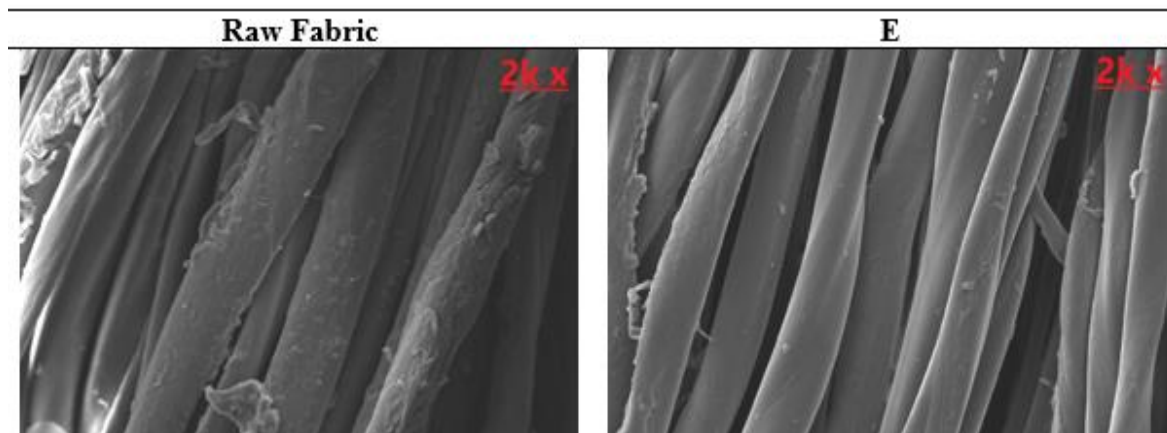


Figure 7:

SEM images of raw fabric (left) and the coated photocured fabric (E) (right).

Figure 8 summarizes the abrasion resistance results along with the wettability properties of raw fabric and coated photocured fabrics by means of contact angle and absorbency tests. The principle of the absorbency test is to observe the water droplet on the coated photocured fabric surfaces and to record the time by a chronometer that is needed for the disappearance of the droplet (Chen, Cai et al. 2019). Accordingly, due to the inherent hydrophilic property of the raw cotton fabric, the contact angle and absorbency test results of the raw fabric were recorded as 39° and 3 seconds, respectively. After coating process, the absorbency times and contact angles all increased due to the existence of a coating layer on cotton fabric that gives a hydrophobic character to the fabric. The synthesized P-ESBO oligomer possesses hydrophilic polar groups (hydroxyl, carbonyl, phosphate) on its backbone that can be interacted with the water molecules (Baker, Drelich et al. 2007). Thus whenever the amount of P-ESBO oligomer increases in the coating formulation, the contact angles and absorbency times decrease. Thus, considering the coated photocured samples, the least disappearance time of the water droplet with 10.4 min and the lowest contact angle value of 85° were observed in the sample of E. Considering the surface wettability property, a hydrophobic surface should demonstrate a contact angle value above 90° (Law 2014), thus almost all samples can be accepted as hydrophobic except sample E. But it is also very close to a hydrophobic character with a contact angle of 85° .

The abrasion resistance test was employed by using Martindale abrasion and pilling device in order to investigate the adhesion between the coating layer and the fabric surface. The principle of the abrasion test is that to calculate the weight loss of samples in 5 cm diameter before abrasion and after abraded by a sandpaper for 100 cycle abrasion (Cai, Chen et al. 2020). This test has been developed by ISO standards just for the rubber/polymer coated fabrics. Thus it cannot be applied on the raw fabric surface. Considering the abrasion resistance test results in Figure 8, the highest weight loss value of 5.7 % after abrasion was observed in the sample of A. The weight loss values decreased gradually to the sample E and the least weight loss value of 2.9 % was recorded in the sample E. This result can be explained by the hydrophilic and flexible groups of the synthesized P-ESBO oligomer which act as an adhesion promoter between the coating layer and the fabric surface (Yildiz, Gungor et al. 2016). Furthermore, the phosphorus group of Sipomer PAM-200 in P-ESBO oligomer also inherently promotes high adhesion properties between the adherent layers (Wehbi, Mehdi et al. 2019). The bonding mechanism between the fabric and the coating layer was illustrated in Figure 9. The abundant hydroxyl groups of cotton fabric are responsible of the formation of several hydrogen bondings between the coating layer and the fabric. The hydrogen bonding associations, in red-dashed lines, were established between the hydroxyl groups of fabric and several functional groups of coating layer such as; $-\text{OH}$ and $\text{P}=\text{O}$ groups of phosphate, carbonyl groups of triglycerides, carbonyl group in methacrylate, and $-\text{OH}$ groups that are formed by the ring opening reaction.

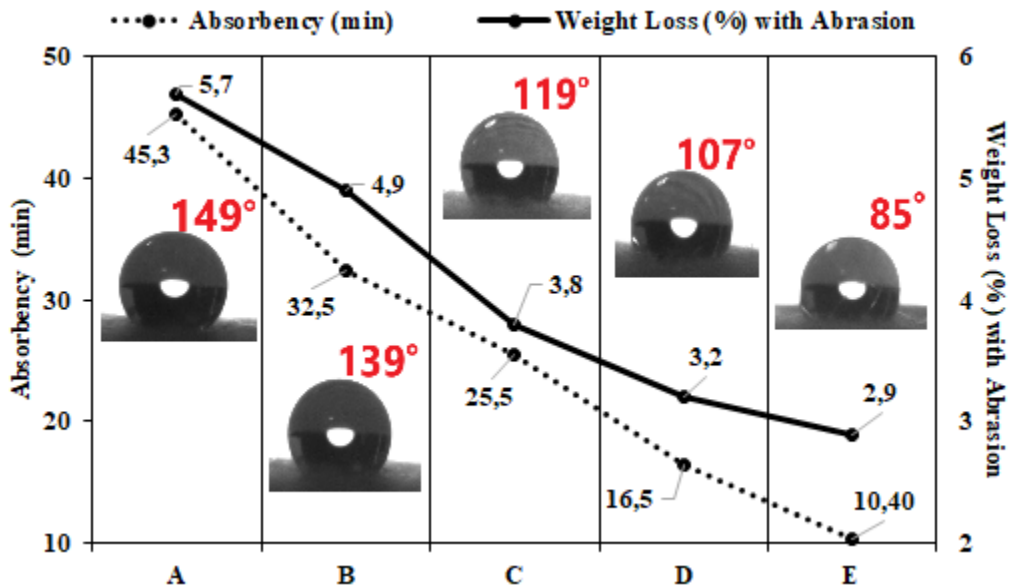


Figure 8:
The contact angles, absorbency times, and weight loss percentages after abrasion for each coated photocured fabric sample.

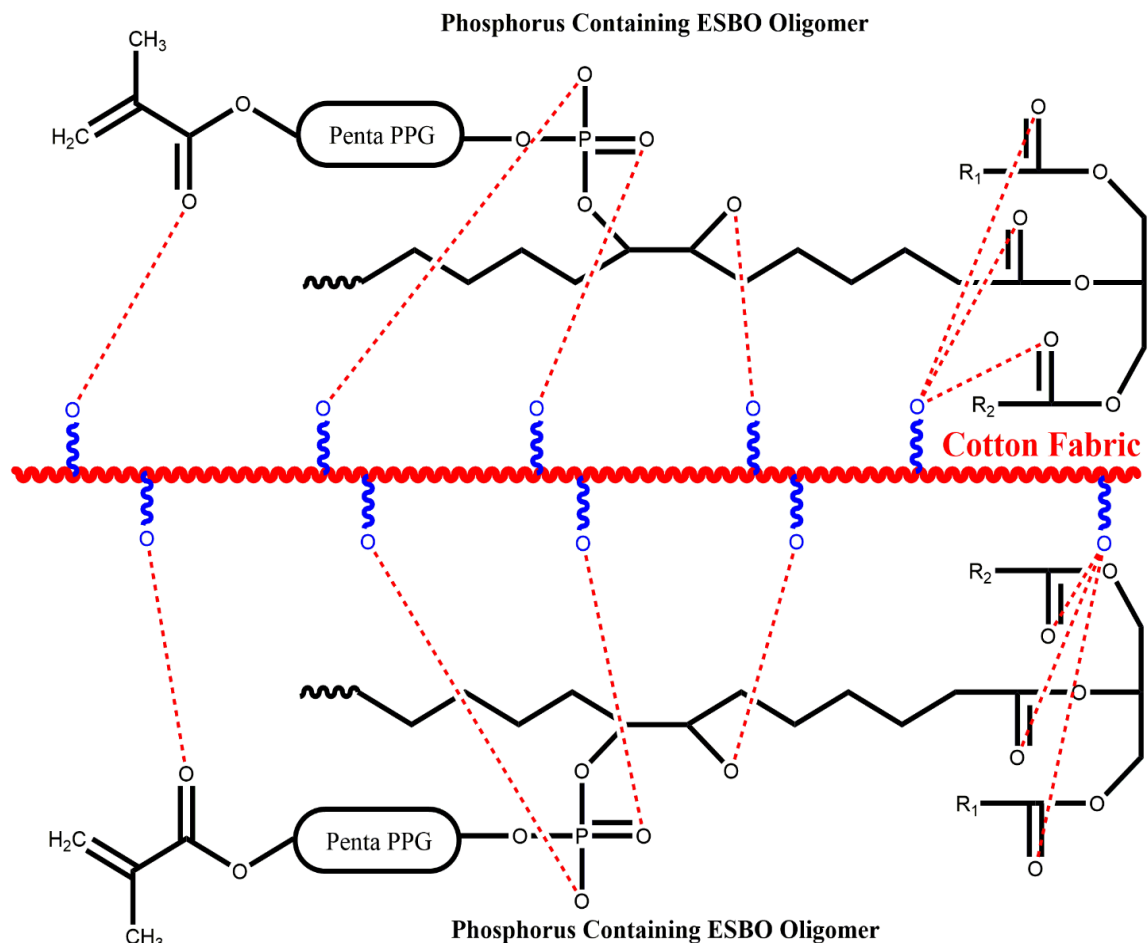


Figure 9:

Scheme of the bonding mechanism between the coating layer and the cotton fabric.

3.6. Mechanical Properties

The mechanical properties of raw fabric and coated photocured fabrics for each formulation by means of tensile testing and crease recovery angle test were illustrated in Table 3. The mechanical behavior of the fabric samples can be explained by considering the chemical structure of the coating formulations. The synthesized P-ESBO oligomer presents much more connection points that can be interacted with the hydroxyl groups of cotton fabric (Gu, Liu et al. 2020). As can be seen in Figure 1 and 9, the carbonyl groups of triglycerides, phosphate ester and carbonyl groups of monomethacrylate functional phosphorus containing monomer, hydroxyl groups formed after the ring opening reaction of epoxide groups are all the potential connection points to the hydroxyl groups of cotton fabric. Whenever the P-ESBO oligomer amount increases in the formulation the tensile strength also increases. Thus the highest tensile strength value was recorded in the sample of E. A similar explanation can be also made for the elongation property. The P-ESBO oligomer has long flexible aliphatic groups (penta PPG; a polyol group) on its backbone. The flexible groups support the ductility nature of the structure resulting an increased elongation at break values. Besides, the pendant methyl groups of PPG inhibit a close packing of polymer chains by increasing the free volume of the chains

and act as internal plasticizer (Kaczmarek and Vuković-Kwiatkowska 2012, Kalita 2018). Due to the mentioned reasons the elongation at break value increases with increasing amount of P-ESBO oligomer in the coating formulation.

The crease recovery angle of a fabric gives idea about the handle and drapeability properties of the fabric. These properties are highly correlated with flexibility and resilience notions. The crease recovery angle gives idea about the flexibility of the fabric by searching the ability of fabric about turning back to the unfolded position when the loading is removed. Accordingly, the raw fabric showed the highest crease recovery angle values in both warp and weft directions due to the flexible property of the fabric. After the coating and photocuring processes, the crease recovery angles decreased in all samples due to the existence of a coating layer on the fabric surface which limits the fiber movements with a partial loss of flexibility property. As mentioned before, the synthesized P-ESBO oligomer has flexible long aliphatic groups (penta PPG) on its backbone and gives resilience property to the fabric surface. Thus, whenever the amount of P-ESBO oligomer increases in the formulation the crease recovery angles also increase. In other words, the sample of E shows the most similarity to the raw cotton fabric in terms of the drapeability and handle characteristics. Lower crease recovery angle means that when a force is applied on fabric, a crimp is formed between the folded parts of fabric which restricts the fabric for turning back to the unfolded position (Abrishami, Mousazadegan et al. 2019, Wang, Fu et al. 2021). Due to the absence of the synthesized P-ESBO oligomer in the sample of A, the lowest crease recovery angles were recorded in that sample.

Table 3. Mechanical testing results of raw fabric and coated photocured fabrics for each formulation.

Sample Codes	Tensile Strength (N)	Elongation at Break (%)	Crease Recovery Angle (°)	
			Warp	Weft
Raw Fabric	893	12.9	84	95
A	1058	13.5	52	56
B	1072	14.7	62	79
C	1081	15.6	67	83
D	1086	15.9	71	85
E	1093	16.2	76	87

4. CONCLUSION

In this work, bio-based phosphorylated photocurable oligomer was synthesized with the reaction between the oxirane ring of ESBO and a monomethacrylate functional phosphorus containing monomer. The synthesized oligomer was included in coating formulations in different proportions and then coating formulations were applied on cotton fabric surfaces and cured by UV-light. This study proves that the inclusion of a phosphorus-based monomer to the oligomer structure enhances the adhesion between the fabric surface and coating layer by improving the abrasion resistance. Due to the existence of connection points between the coating layer and the cotton fabric which were constituted by the phosphate ester and carbonyl groups in monomethacrylate functional phosphorus containing oligomer, carbonyl groups of triglycerides in ESBO, and hydroxyl groups formed after the ring opening reaction of epoxide groups, the tensile strength and adhesion increased with increasing P-ESBO oligomer in the coating formulation. Furthermore, higher char yield and LOI values were recorded with increasing amount of phosphorylated oligomer in the formulation, that can prevent fire propagation on the coated photocured cotton fabric surfaces. The designed coated cotton fabrics (172

g/m² in weight with 1093 N tensile strength) here, can be accepted as an alternative compared to the conventional tarpaulin materials (500-850 g/m² in weight with 900-1500 N tensile strength on average) since they present several advantages such as being lightweight, manufacturing via solvent-/waterless, time/energy saving photocuring technique, presenting a hydrophobic and partial flame resist property.

ACKNOWLEDGEMENT

I would like to present my special thanks to Prof. Dr. Atilla Gungor, who was a very valuable scientist in chemistry world and unfortunately no longer with us, for his great contributions on my polymer knowledge. I would also like to thank Ms. Ovgu Gurer (M. Sc.) and Ms. Sevval Kar (B. Sc.) for their assistantship on the experimental study. I am also pleased to acknowledge Kadifeteks Mensucat Co. Inc. for their kind assistance in LOI test.

CONFLICT OF INTEREST

The author declares that she has no known competing financial interests or personal relationships that could have appeared to influence the work reported in this paper.

AUTHOR CONTRIBUTION

Zehra Yildiz: Literature Review, Investigation, Writing, Visualization, and Editing.

REFERENCES

1. AATCC Test Method 79-2018: Absorbency of Bleached Textiles," ed, 2018.
2. ASTM D974-14e2, Standard Test Method for Acid and Base Number by Color-Indicator Titration, ASTM International, West Conshohocken, PA, 2014, www.astm.org. doi:10.1520/D0974-14E02
3. ASTM D1652-11(2019), Standard Test Method for Epoxy Content of Epoxy Resins, ASTM International, West Conshohocken, PA, 2019, www.astm.org. doi: 10.1520/D1652-11R19
4. ISO 5470-2:2003 Rubber- or plastics-coated fabrics — Determination of abrasion resistance Part 2: Martindale abrader.
5. ISO 13934-1:2013 Textiles — Tensile properties of fabrics — Part 1: Determination of maximum force and elongation at maximum force using the strip method.
6. ASTM D2863-19:2019 Standard Test Method for Measuring the Minimum Oxygen Concentration to Support Candle-Like Combustion of Plastics (Oxygen Index). doi: 10.1520/D2863-19
7. Abrishami, S., F. Mousazadegan and N. Ezazshahabi (2019). "Evaluating the crease recovery performance of woven fabrics considering bending behaviour in various directions." *The Journal of the Textile Institute* 110(5): 690-699. doi: 10.1080/00405000.2018.1511229
8. Alam, M., D. Akram, E. Sharmin, F. Zafar and S. Ahmad (2014). "Vegetable oil based eco-friendly coating materials: A review article." *Arabian Journal of Chemistry* 7(4): 469-479. doi: 10.1016/j.arabjc.2013.12.023

9. Aliverdipour, N., N. Ezazshahabi and F. Mousazadegan (2020). "Characterization of the effect of fabric's tensile behavior and sharp object properties on the resistance against penetration." *Forensic science international* 306: 110097. doi: 10.1016/j.forsciint.2019.110097
10. Bajpai, M., V. Shukla and A. Kumar (2002). "Film performance and UV curing of epoxy acrylate resins." *Progress in Organic Coatings* 44(4): 271-278. doi: 10.1016/S0300-9440(02)00059-0
11. Baker, K., J. Drelich, I. Miskioglu, R. Israel and H. Herkowitz (2007). "Effect of polyethylene pretreatments on the biomimetic deposition and adhesion of calcium phosphate films." *Acta biomaterialia* 3(3): 391-401. doi: 10.1016/j.actbio.2006.08.008
12. Baştürk, E., T. İnan and A. Güngör (2013). "Flame retardant UV-curable acrylated epoxidized soybean oil based organic-inorganic hybrid coating." *Progress in Organic Coatings* 76(6): 985-992. doi: 10.1016/j.porgcoat.2012.10.007
13. Cai, L., C. Chen, W. Wang, X. Gao, X. Kuang, Y. Jiang, L. Li and G. Wu (2020). "Acid-free epoxidation of soybean oil with hydrogen peroxide to epoxidized soybean oil over titanium silicalite-1 zeolite supported cadmium catalysts." *Journal of Industrial and Engineering Chemistry* 91: 191-200. doi: 10.1016/j.jiec.2020.07.052
14. Chen, C., L. Cai, L. Li, L. Bao, Z. Lin and G. Wu (2019). "Heterogeneous and non-acid process for production of epoxidized soybean oil from soybean oil using hydrogen peroxide as clean oxidant over TS-1 catalysts." *Microporous and Mesoporous Materials* 276: 89-97. doi: 10.1016/j.micromeso.2018.09.028
15. Chen, L., L. Song, P. Lv, G. Jie, Q. Tai, W. Xing and Y. Hu (2011). "A new intumescent flame retardant containing phosphorus and nitrogen: Preparation, thermal properties and application to UV curable coating." *Progress in Organic Coatings* 70(1): 59-66. doi: 10.1016/j.porgcoat.2010.10.002
16. Chen, Y., L. Yang, J. Wu, L. Ma, D. E. Finlow, S. Lin and K. Song (2013). "Thermal and mechanical properties of epoxy resin toughened with epoxidized soybean oil." *Journal of thermal analysis and calorimetry* 113(2): 939-945. doi: 10.1007/s10973-012-2859-4
17. Çakmakçı, E. (2017). "Allylamino diphenylphosphine oxide and poss containing flame retardant photocured hybrid coatings." *Progress in Organic Coatings* 105: 37-47. doi: 10.1016/j.porgcoat.2016.11.013
18. Gan, L. (2021). Production and application of fine powder from textile waste (Doctoral dissertation, Institute for Frontier Materials, Deakin University, Australia).
19. Gao, M., W. Wu and F. Wu (2009). "Thermal degradation and smoke suspension of cotton cellulose modified with THPC and its lanthanide metal complexes." *Journal of thermal analysis and calorimetry* 98(1): 245-251. doi: 10.1007/s10973-009-0122-4
20. Gong, K., K. Zhou and B. Yu (2020). "Superior thermal and fire safety performances of epoxy-based composites with phosphorus-doped cerium oxide nanosheets." *Applied Surface Science* 504: 144314. doi: 10.1016/j.apsusc.2019.144314
21. Gu, W., X. Liu, Q. Gao, S. Gong, J. Li and S. Q. Shi (2020). "Multiple hydrogen bonding enables strong, tough, and recyclable soy protein films." *ACS Sustainable Chemistry & Engineering* 8(20): 7680-7689. doi: 10.1021/acssuschemeng.0c01333

22. Gupta, P., V. Uniyal and S. Naithani (2013). "Polymorphic transformation of cellulose I to cellulose II by alkali pretreatment and urea as an additive." *Carbohydrate polymers* 94(2): 843-849. doi: 10.1016/j.carbpol.2013.02.012
23. Habib, F. and M. Bajpai (2010). "UV Curable heat resistance Epoxy Acrylate Coatings." *Journal of Chemistry & Chemical Technology* 4(3): 205-216. doi: 10.23939/chcht04.03.205
24. Hwang, J.-S., M.-H. Kim, D.-S. Seo, J.-W. Won and D.-K. Moon (2009). "Effects of soft segment mixtures with different molecular weight on the properties and reliability of UV curable adhesives for electrodes protection of plasma display panel (PDP)." *Microelectronics Reliability* 49(5): 517-522. doi: 10.1016/j.microrel.2009.02.001
25. Islam, M. R., M. D. H. Beg and S. S. Jamari (2014). "Development of vegetable-oil-based polymers." *Journal of applied polymer science* 131(18). doi: 10.1002/app.40787
26. Kaczmarek, H. and I. Vuković-Kwiatkowska (2012). "Preparation and characterization of interpenetrating networks based on polyacrylates and poly (lactic acid)." *eXPRESS Polymer Letters* 6(1). doi: 10.3144/expresspolymlett.2012.9
27. Kalita, H. (2018). 4. Shape memory polyurethanes: From materials to synthesis. *Shape Memory Polymers*, De Gruyter: 103-120. doi: 10.1515/9783110570175-004
28. Kowalczyk, A., K. Kowalczyk and M. Weisbrodt (2018). "Influence of a phosphorus-based methacrylate monomer on features of thermally curable self-adhesive structural tapes." *International Journal of Adhesion and Adhesives* 85: 286-292. doi: 10.1016/j.ijadhadh.2018.07.002
29. Law, K. Y. (2014). Definitions for hydrophilicity, hydrophobicity, and superhydrophobicity: getting the basics right. *The Journal of Physical Chemistry Letters*, 5(4), 686-688. doi: 10.1021/jz402762h
30. Li, P., S. Ma, J. Dai, X. Liu, Y. Jiang, S. Wang, J. Wei, J. Chen and J. Zhu (2017). "Itaconic acid as a green alternative to acrylic acid for producing a soybean oil-based thermoset: synthesis and properties." *ACS Sustainable Chemistry & Engineering* 5(1): 1228-1236. doi: 10.1021/acssuschemeng.6b02654
31. Liu, H., K. Xu, H. Cai, J. Su, X. Liu, Z. Fu and M. Chen (2012). "Thermal properties and flame retardancy of novel epoxy based on phosphorus-modified Schiff-base." *Polymers for Advanced Technologies* 23(1): 114-121. doi: 10.1002/pat.1832
32. Liu, R., J. Luo, S. Ariyasivam, X. Liu and Z. Chen (2017). "High biocontent natural plant oil based UV-curable branched oligomers." *Progress in Organic Coatings* 105: 143-148. doi: 10.1016/j.porgcoat.2016.11.009
33. Liu, Z., L. Wang, C. Bao, X. Li, L. Cao, K. Dai and L. Zhu (2011). "Cross-linked PEG via degradable phosphate ester bond: synthesis, water-swelling, and application as drug carrier." *Biomacromolecules* 12(6): 2389-2395. doi: 10.1021/bm2004737
34. Luangtriratana, P., B. K. Kandola and J. R. Ebdon (2015). "UV-polymerisable, phosphorus-containing, flame-retardant surface coatings for glass fibre-reinforced epoxy composites." *Progress in Organic Coatings* 78: 73-82. doi: 10.1016/j.porgcoat.2014.10.004

35. Moon, J., Y. Shul, H. Han, S. Hong, Y. Choi and H. Kim (2005). "A study on UV-curable adhesives for optical pick-up: I. Photo-initiator effects." *International journal of adhesion and adhesives* 25(4): 301-312. doi: 10.1016/j.ijadhadh.2004.09.003
36. Nam, S., A. D. French, B. D. Condon and M. Concha (2016). "Segal crystallinity index revisited by the simulation of X-ray diffraction patterns of cotton cellulose I β and cellulose II." *Carbohydrate polymers* 135: 1-9. doi: 10.1016/j.carbpol.2015.08.035
37. Rowe, M. C. and B. J. Brewer (2018). "AMORPH: A statistical program for characterizing amorphous materials by X-ray diffraction." *Computers & geosciences* 120: 21-31. doi: 10.1016/j.cageo.2018.07.004
38. Salim, T. A., N. H. Abas, S. Shahidan, R. Deraman, M. F. Hasmori, S. Nagapan, T. Y. Ghing and N. Ain (2018). "Investigation on the Influence of Non-Degradable Polyvinyl Tarpaulin in Concrete Mixture." *Sustainable Construction and Building Technology*: 71-82. ISBN 978-967-2216-39-1
39. Shi, L.-S., L.-Y. Wang and Y.-N. Wang (2006). "The investigation of argon plasma surface modification to polyethylene: Quantitative ATR-FTIR spectroscopic analysis." *European Polymer Journal* 42(7): 1625-1633. doi: 10.1016/j.eurpolymj.2006.01.007
40. Su, Y.-C., L.-P. Cheng, K.-C. Cheng and T.-M. Don (2012). "Synthesis and characterization of UV-and thermo-curable difunctional epoxyacrylates." *Materials Chemistry and Physics* 132(2-3): 540-549. doi: 10.1016/j.matchemphys.2011.11.067
41. Sung, S. and D. S. Kim (2013). "UV-curing and mechanical properties of polyester-acrylate nanocomposites films with silane-modified antimony doped tin oxide nanoparticles." *Journal of applied polymer science* 129(3): 1340-1344. doi: 10.1002/app.38824
42. Ugur, M., H. Kılıç, M. Berkem and A. Güngör (2014). "Synthesis by UV-curing and characterisation of polyurethane acrylate-lithium salts-based polymer electrolytes in lithium batteries." *Chemical Papers* 68(11): 1561-1572. doi: 10.2478/s11696-014-0611-1
43. Uysal, N., G. Acik and M. A. Tasdelen (2017). "Soybean oil based thermoset networks via photoinduced CuAAC click chemistry." *Polymer International* 66(7): 999-1004. doi: 10.1002/pi.5346
44. Wang, K., C. Fu, R. Wang, G. Tao and Z. Xia (2021). "High-resilience cotton base yarn for anti-wrinkle and durable heat-insulation fabric." *Composites Part B: Engineering* 212: 108663. doi: 10.1016/j.compositesb.2021.108663
45. Wehbi, M., A. Mehdi, C. Negrell, G. David, A. Alaaeddine and B. Ameduri (2019). "Phosphorus-containing fluoropolymers: State of the art and applications." *ACS applied materials & interfaces* 12(1): 38-59. doi: 10.1021/acsami.9b16228
46. Wu, Q., Y. Hu, J. Tang, J. Zhang, C. Wang, Q. Shang, G. Feng, C. Liu, Y. Zhou and W. Lei (2018). "High-performance soybean-oil-based epoxy acrylate resins: "Green" synthesis and application in uv-curable coatings." *ACS Sustainable Chemistry & Engineering* 6(7): 8340-8349. doi: 10.1021/acssuschemeng.8b00388
47. Wu, Y., A. Liu, W. Li and Z. Li (2019). "Synthesis of carborane acrylate and flame retardant modification on silk fabric via graft copolymerization with phosphate-containing acrylate." *Fire and Materials* 43(7): 880-891. doi: 10.1002/fam.2748

48. Xu, L., W. Wang and D. Yu (2017). "Preparation of a reactive flame retardant and its finishing on cotton fabrics based on click chemistry." *RSC advances* 7(4): 2044-2050. doi: 10.1039/C6RA26075F
49. Yang, Z., Z. Zeng, Z. Xiao and H. Ji (2014). "Preparation and controllable release of chitosan/vanillin microcapsules and their application to cotton fabric." *Flavour and fragrance journal* 29(2): 114-120. doi: 10.1002/ffj.3186
50. Yildiz, Z. (2023). "Photocurable soybean oil based phosphorus containing coatings for cotton fabrics: The influence of reactive diluents." *Progress in Organic Coatings* 174: 107255. doi: 10.1016/j.porgcoat.2022.107255
51. Yildiz, Z., A. Gungor, A. Onen and I. Usta (2016). "Synthesis and characterization of dual-curable epoxyacrylates for polyester cord/rubber applications." *Journal of Industrial Textiles* 46(2): 596-610. doi: 10.1177/1528083715594980
52. Yildiz, Z., A. Onen and A. Gungor (2016). "Preparation of flame retardant epoxyacrylate-based adhesive formulations for textile applications." *Journal of adhesion science and Technology* 30(16): 1765-1778. doi: 10.1080/01694243.2016.1159036
53. Zhang, C., T. F. Garrison, S. A. Madbouly and M. R. Kessler (2017). "Recent advances in vegetable oil-based polymers and their composites." *Progress in Polymer Science* 71: 91-143. doi: 10.1016/j.progpolymsci.2016.12.009

